AIAA Aviation
16-20 June 2014, Atlanta, GA
20th AIAA/CEAS Aeroacoustics Conference

Simulations of Acoustic Wave Propagation in an Impedance Tube Using a Frequency-Domain Linearized Navier-Stokes Methodology

W. Na* and S. Boij †

Linne FLOW Centre, KTH Aeronautical and Vehicle Engineering, Stockholm, Sweden

G. Efraimsson ‡

Centre for ECO^2 Vehicle Design, KTH Aeronautical and Vehicle Engineering, Stockholm, Sweden

In this paper, we present analysis of the propagation of acoustic plane waves in an impedance tube, in which a liner is attached at one end of the duct. The purpose is to evaluate a linearized Navier-Stokes solver as a tool to determine the acoustic performance of the liner. The liner considered consists of a perforated plate with several circular holes and a rectangular back cavity. The influence of parameter variations such as plate thickness, porosity area examined.

The prediction of the acoustic characters of the liner is based on the numerical solutions of the linearized Navier-Stokes equations in frequency domain in three space dimensions. The impedance as well as reflection coefficients of the liner for frequencies in the plane wave regime are obtained by two-microphone method data, which are compared to experimental data as well as results from a semi-empirical model. The results presented in this paper agree very well with results of the linear semi-empirical model, while there are some discrepancies to the experimental results. The reasons for these discrepancies are not fully understood, but could partly be due to that a linear assumption is not always valid.

I. Introduction

Liners are a standard mean to reduce engine noise in today's aeroengines. In order to optimize the design of the liner, it is essential to be able to predict the acoustic performance of the liner already in the design phase of the aero-engine. Hence, accurate and efficient prediction tools are of vital interest.

A liner typically consists of a perforated plate with small holes. The dissipation in the acoustic boundary layer has a strong damping effect on the acoustic waves in the small sized holes, which are typically around 1 mm in diameter. When the perforated plate is mounted on to a cavity, the phase of the incident wave is changed due to the reflection caused by surrounding walls of cavity. Large amplitudes will appear at the Helmholtz resonance frequency of the cavity which will enhance the acoustic dissipation at this frequency.

The impedance of a liner is in general determined primarily via semi-empirical models and experiments. However, the use of the semi-empirical models is still demanding, when significant changes in the liner structure are made, implying that the prediction of liner impedance becomes less reliable.[1] The impedance of a liner within an impedance tube can be determined experimentally in several ways. One way is to use a two-microphone technique, such as that discussed by Bodén and Åbom[2,3] In this paper, the same two-microphone technique is used to calculate the impedance from the numerical results.

In a series of papers, Tam et al[4,5] studies damping of acoustic waves in a perforated liner using direct numerical simulation(DNS). It is found that the viscous effects are dominant in the vicinity of the wall of the holes in the perforated plate, while the compressibility effect is dominant further away from the wall. By solving the compressible Naiver-stokes equations in time domain, Zhang and Bodony[6] performed

*PhD Candidate.
†Associate professor and AIAA Member.
‡Professor and AIAA Member.

DNS simulations of acoustic waves through a circle orifice that is backed by a hexagonal cavity, where two time-domain models for the orifice fluid velocity were presented.

For design purposes it would be of interest to have a simulation methodology which is less computationally expensive than DNS or Large Eddy Simulations (LES). For this purpose, the frequency-domain linearized Navier-Stokes methodology is evaluated in this paper as a tool to determine the impedance of a liner in an impedance tube . Under the assumption of linear acoustics, it has potential to be a useful tool for simulations of the acoustic properties of liners since viscous dissipation is included in the governing equations. The primary objective of this paper is to evaluate the use of a linearized Navier-Stokes solver to be used for predictions for the impedance of a liner consisting of a perforated plate and a back cavity which is placed in an impedance tube. Another objective is to investigate the influence of the liner perforation and thickness of the perforated plate for a frequency range of plane acoustic waves. The numerical results are compared to experimental data obtained at KTH, see Kabral et al.[7]

The paper is organized as follows. In Sec II the geometry of the liner is described, followed by a presentation of the linearized Navier-Stokes equations as well as the numerical setup and post processing technique used in Sec III. In Sec IV a semi-empirical model, which is used for comparison, is described. The numerical results and the comparison to experimental and theoretical results are presented in Sec V followed by conclusions.

II. Liner geometry

The liner investigated in this paper consists of a rectangular cavity and a perforated plate with circular holes mounted on top of the cavity. The key parameters involved in determining the acoustic impedance of the liner are the diameter of the circular holes of the perforated plate, plate thickness, perforation ratio, as well as the dimension of the cavity.

Fig 1 shows the geometry of the hybrid liner. As shown in the figure, each cavity is covered by a segment of the perforated plate with several small holes. Plates with two different number of holes per cavity are investigated, 6 and 9 holes, with the same hole diameter of the single hole $\phi = 1.5mm$. This in turn yields a porosity 22% and 33%, respectively. The simulated results are compared to measured data[7] where the number of holes per cell matches exactly the number of holes per cell in experiments.

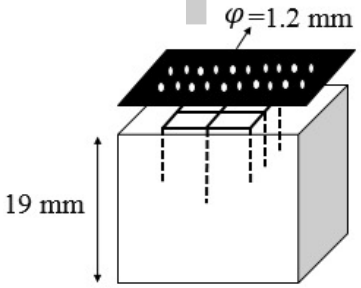

Figure 1. The schematic of the liner geometry

III. Governing equations, numerical setup and post-processing

A modeling framework for solving the linearized Navier-Stokes equations in 2D cartesian coordinates or axisymmetric cylindrical coordinates was developed by Kierkegaard et al.[8–10] Later on, the methodology was extended to 3D cartesian coordinates[11,12] and initial simulations of the acoustic properties of a perforated liner were performed. In the present paper simulation results compared with detailed experimental data, measured at KTH, for acoustic wave propagation in an impedance tube.[7]

The linearized Navier-Stokes equations are derived from the full compressible Navier-Stokes equations. For clarity, we include a brief description here. The current implementation of the frequency domain lin-

earized Navier-Stokes equations can be written as:

$$-i\omega\hat{\rho} + \mathbf{u}_0 \cdot \nabla\hat{\rho} + \hat{\mathbf{u}} \cdot \nabla\rho_0 + \rho_0 \nabla \cdot \hat{\mathbf{u}} + \hat{\rho}\nabla \cdot \mathbf{u}_0 = 0 \tag{1}$$

$$\begin{aligned} -i\omega\rho_0\hat{\mathbf{u}} + \rho_0(\mathbf{u}_0 \cdot \nabla)\hat{\mathbf{u}} + \rho_0(\hat{\mathbf{u}} \cdot \nabla)\mathbf{u}_0 + \hat{\rho}(\mathbf{u}_0 \cdot \nabla)\mathbf{u}_0 = \\ -c^2\nabla\hat{\rho} + \mu(\nabla^2\hat{\mathbf{u}} + \frac{1}{3}\nabla(\nabla \cdot \hat{\mathbf{u}})) + \nabla\mu\cdot(\nabla\hat{\mathbf{u}} + (\nabla\hat{\mathbf{u}})^T) - \frac{2}{3}(\nabla \cdot \hat{\mathbf{u}})\nabla\mu + \rho_0\hat{\mathbf{F}} \end{aligned} \tag{2}$$

where a hat $\hat{}$ indicates a perturbed quantity, a subscript zero indicates mean flow quantities, ρ is the density, $\mathbf{u}$ is the velocity vector, $\mathbf{F}$ is a volume force, ω is the angular frequency, c is the speed of sound and μ is the kinematic viscosity.

A frequency domain approach has been taken by prescribing harmonic time-dependence of the perturbed quantities. In this way, any perturbed quantity $q^{'}$ can be represented as $q^{'}(x,\omega,t) = Re\left\{\hat{q}(x)e^{-i\omega t}\right\}$, where $\hat{q}$ is a complex quantity and ω is the angular frequency.

Furthermore, an isentropic relation between pressure and density is assumed in Eqs. (1-2), that is

$$\frac{\partial\hat{p}}{\partial x_i} = c^2\frac{\partial\hat{\rho}}{\partial x_i} \tag{3}$$

where $c^2(x) = \gamma p_0/\rho_0$ is the local adiabatic speed of sound, and γ is the ratio of specific heats. With this relation, the fluctuating pressure becomes redundant and can be removed from the system, and the continuity and momentum equations are decoupled from the energy equation. In this way, the size of the computational problem is considerably reduced.

The following boundary conditions are used in simulations. At the impedance tube walls, a rigid wall slip boundary condition is imposed in the longitudinal direction as

$$\hat{u} \cdot \hat{n} = 0, \hat{n} \cdot \nabla\hat{\rho} = 0, \tag{4}$$

In the vicinity of walls of circular holes, rigid wall no-slip boundary conditions are applied as

$$\hat{u} = 0, \hat{n} \cdot \nabla\hat{\rho} = 0. \tag{5}$$

where $\hat{n}$ is the unit vector normal to the walls.

The viscosity in the whole numerical zones can be written as

$$\mu = \mu_{physical} + \mu_{artifical} \tag{6}$$

where $\mu_{artifical} = 0$ and $\mu_{physical} = 1e^{-5}$ at the solid boundaries. Buffer zones are used to damp out the acoustic waves, in the buffer zones, the $\mu_{artifical}$ is ramped up as a cubic polynomial through the buffer zone to a specific value, in this case, $\mu_{artifical} = 10$.

The simulations are carried out in COMSOL 4.3a, which is a commercial finite element method (FEM) solver. The numerical model also includes the possibility to include a metal foam via the use of the Delany-Bazley model, see Kierkegaard et al[11] for further details.

A. Numerical setup

A schematic of the geometry in the calculation is shown in Fig 2. Compared with the full duct length of the experimental rig, see Kabral[7] for further details, the duct length used in the acoustic simulations is around 0.7m to reduce computational costs. Both of the height and the width of the duct is $6.9mm$, it equals to the dimension of the single cavity.

At the upper end of the impedance tube, a buffer zone is placed in the simulations to avoid reflections. The incident plane wave is placed as a body force in momentum equation in the buffer zone. The mesh used in simulations is unstructured prism mesh with about 210000 elements, the overview mesh and the mesh in the vicinity of the perforated plate is shown in figure 3. The sound excitation is the plane wave from $1500Hz$ to $5500Hz$ yielding that the maximum wavelength of the acoustic wave is $226.7mm$ and the minimum wavelength is $7.2mm$, with a grid element size $1mm$, there are 7 elements per wavelength for the high frequency.

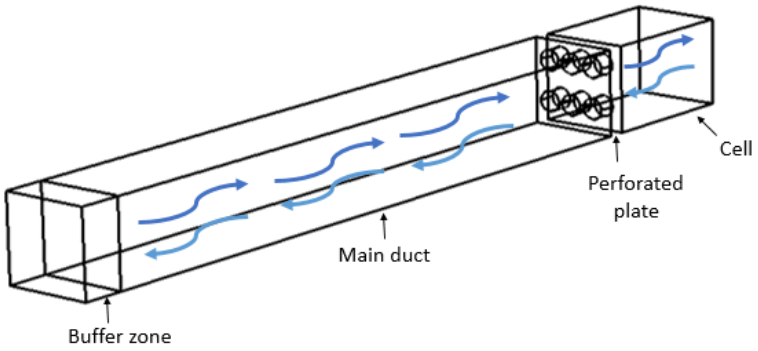

Figure 2. Schematic sketch of the numerical model of impedance tube

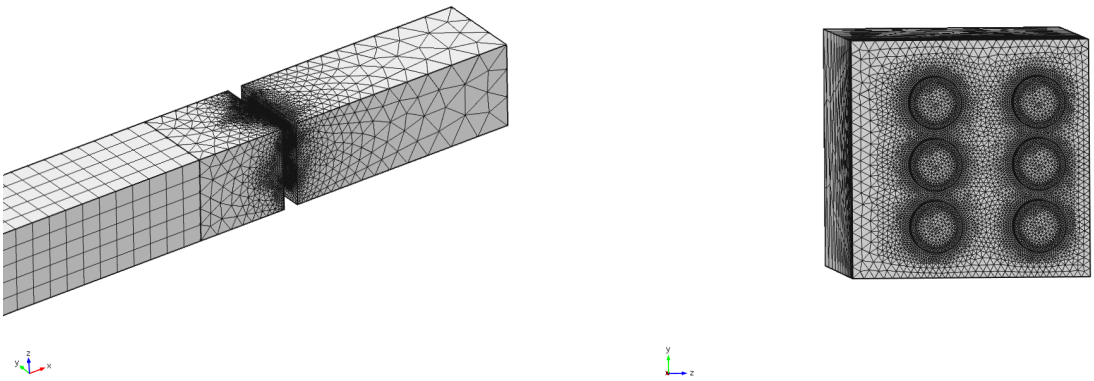

(a) Overview of the mesh for the impedance tube

(b) The mesh shown in the vicinity of the perforated plate

Figure 3. Overview of the mesh for the acoustic field

B. Post-process: two-microphone technique

In order to characterize the acoustic performance of the liner, the impedance and the reflection coefficient is calculated from the numerical results. In the straight cylindrical duct the sound field below the cut-on frequency will consist only of plane waves. In the frequency domain, the sound field can then be written as[13]

$$\hat{p}(x,f) = \hat{p}_+(f)exp(-ik_+x) + \hat{p}_-(f)exp(ik_-x) \tag{7}$$

where $\hat{p}$ is the Fourier transform of the acoustic pressure, x is the coordinate along the duct axis, f is the frequency, k is the complex wave number $\pm$ denotes propagation in positive and negative x-direction, r is the density and c is the speed of sound.

By assuming the complex wavenumbers are known in the duct, the incident and reflected wave amplitude $\hat{p}_+$ and $\hat{p}_-$ can be calculated using two microphone positions as shown in Fig 4

$$\hat{p}_1 = \hat{p}_+(f) + \hat{p}_-(f) \tag{8}$$

$$\hat{p}_2 = \hat{p}_+(f)exp(-ik_+s) + \hat{p}_-(f)exp(ik_-s) \tag{9}$$

where s represents the microphone separation. Eqs. (8) and (9) imply that

$$\hat{p}_+(f) = \frac{\hat{p}_1(f)exp(ik_-s) - \hat{p}_2(f)}{exp(ik_-s) - exp(-ik_+s)} \tag{10}$$

$$\hat{p}_-(f) = \frac{-\hat{p}_1(f)exp(-ik_+s) + \hat{p}_2(f)}{exp(ik_-s) - exp(-ik_+s)} \tag{11}$$

Figure 4. Simulation and measurement configuration for the two-microphone method

IV. A semi-empirical impedance model

In this paper, the simulated normalized impedance of the liner is compared to the results of a semi-empirical model. The normalized impedance is defined as the ratio of impedance and the characteristic impedance[14]

$$z = Z_s/Z_c = r + j\chi \tag{12}$$

where Z_s is the specific impedance, $Z_c = \rho_0 c_0$ is the characteristic impedance of air, where ρ_0 is density of air and c_0 is the speed of sound. The real part r is refered to the resistance, while the imaginary part χ is refered to the reactance.

There exists a number of empirical and semi-empirical model for the acoustic impedance of perforated plates with circular holes, in the absence of the mean flow. In this paper we will use the model proposed by Bauer,[15] where the normalized impedance for an circular orifice without flow is expressed as

$$z = \left[\left(\frac{\sqrt{8\mu\rho_0\omega}}{\rho_0 c_0 \sigma}\right)\left(1 + \frac{t}{d}\right)\right] + j\left[\frac{k(t + 0.25d)}{\sigma}\right]. \tag{13}$$

Here, $\rho_0 c_0$ is the characteristic impedance of the medium, μ is the viscosity coefficient of the medium, σ is the porosity of the perforated plate, d is the diameter of circular holes, t is the thickness of the perforated plate, ω is the circular frequency and k is the wave number.

The resistance of the liner is only determined by the perforated plate, while the reactance consists of two parts, one part due to the perforated plate and the other by the cavity. The reactance of the cavity is

$$\chi_{cavity} = -cot(kH) \tag{14}$$

where k is wave number and H is the depth of the cavity. Hence, a model for the resistance and reactance by semi-empirical model for the impedance of a liner can be expressed as

$$r = \left[\left(\frac{\sqrt{8\mu\rho_0\omega}}{\rho_0 c_0 \sigma}\right)\left(1 + \frac{t}{d}\right)\right] \tag{15}$$

$$\chi = -cot(kH) + \left[\frac{k(t + 0.25d)}{\sigma}\right] \tag{16}$$

V. Results

In this section we present the results of the numerical simulations using the linearized Navier-Stokes equations methodology as described in Sec III. The impedance and the reflection coefficient of the liner in a quiescent medium is compared to results from an semi-empirical model and experiments. The sound excitation is the plane wave from $1500Hz$ to $5500Hz$. The liners response to variations in parameters such as the porosity and the thickness of the plate are presented.

First, in order to check the influence of the grid resolution on the numerical results, simulations for two different mesh sizes were carried out. The results from the semi-empirical model in in Sec IV are also shown. With the finer mesh, the mesh was particularly refined in the regions close to the solid walls in the the vicinity of the perforated plate. The results are shown in Fig 5. There is only small differences between different meshes where the results obtained with finer mesh is closer to the semi-empirical results. For the grid with a lower resolution of the acoustic boundary layer the resistance is lower than for the finer grid and the semi-empirical model while higher values are obtained for the reflection coefficient. However, these differences are of the order of a few percent. The finer grid is used in all simulations presented below.

In Fig 6 the resistance, reactance and the magnitude and phase of the reflection coefficient as a function of frequency are presented together with the results from the semi-empirical model in Sec IV as well as experimental data. The numerical results agree very well with the semi-empirical model. The resistance obtained from the simulations is lower than experimental results while the reactance of impedance agrees perfectly with the semi-empirical model. In the region for small values of the reactance the agreement is excellent with the experimental results, indicating that the simulation tool is able to predict the region of interest for the resonance frequency of the liner. The discrepancy between the experimental and numerical results in the resistance indicate that the dissipation due to viscous effects is larger in the experiments compared to what is obtained in the simulations. One possible explanation could be that nonlinear effects are present in the experiments, while the current numerical solver used in this paper is limited to linear acoustics. This possible explanation is supported by the fact the the simulated data agrees very well with the linear semi-empirical model. However, further studies are needed to sort out the reason for these discrepancies.

In Fig 7 the impedance and reflection coefficients for two different thicknesses of the perforated plate are shown. The thickness of the plates were $0.6mm$ and $1.2mm$, respectively. It is seen that with a thinner perforated plate, the impedance of the perforated plate is lower than for the thicker one which can also be seen in the experimental results and semi-empirical results. In general, the shift in amplitude of the reflection coefficient due to the two plate thicknesses seen in the experiments is captured in the simulations. As for the thicker plate, there is an excellent agreement between the simulated and experimental results in the region of small values of the reactance also for the thinner plate.

Finally, a comparison between perforated plates with different porosities namely with 22.27% and 33.3%, respectively were performed. The liner geometry with the porosity 22.27% corresponds to a 6 holes in the perforated plate, and the porosity 33.3% was obtained through a plate with 9 holes in the perforated plate. The same hole diameter, $\phi = 1.5mm$, was used for the different plates. The grid used has the same resolution for the 9 hole geometry as for the 6 hole geometry. As for the variance in plate thickness, it can be seen that the numerical solver is capable of capturing the difference in amplitude due to the different porosities.

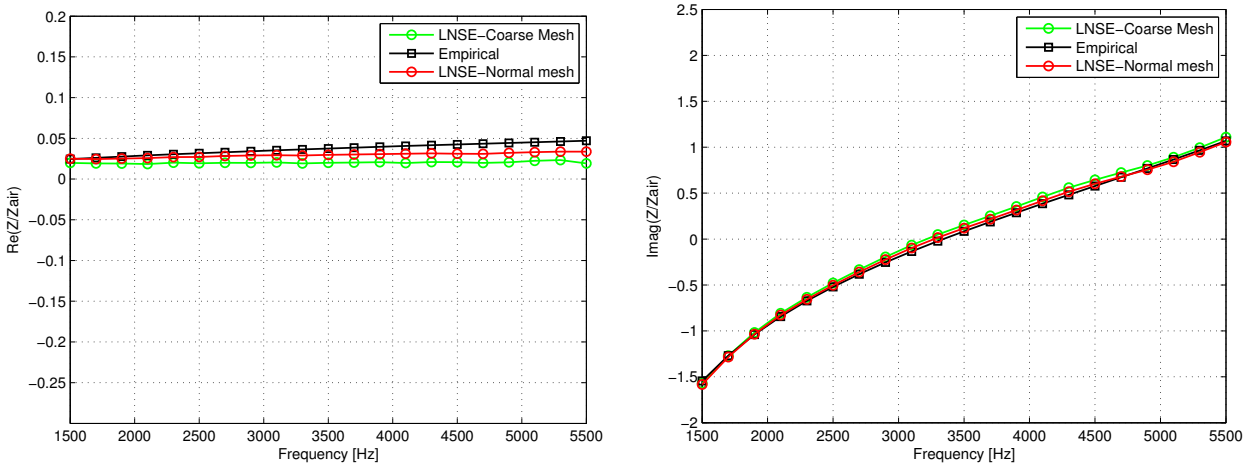

(a) resistance of impedance

(b) reactance of impedance

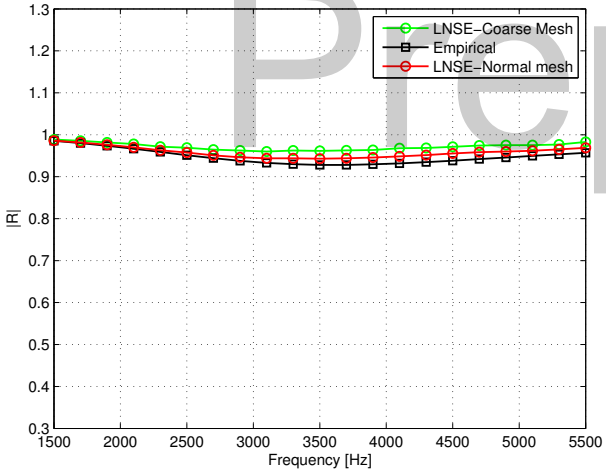

(c) magnitude of reflection coefficient

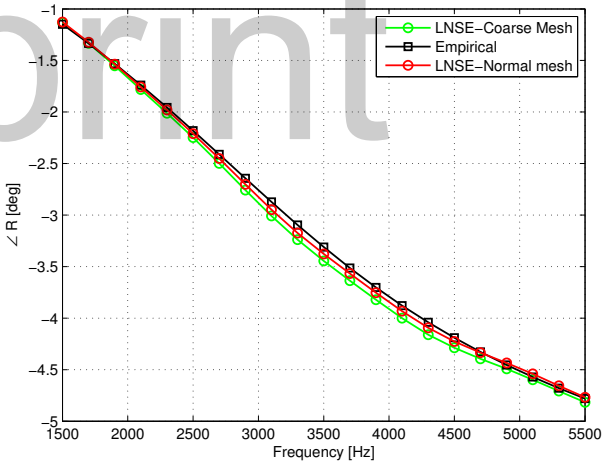

(d) phase of reflection coefficient

Figure 5. Resistance (upper left), reactance (upper right) and the magnitude (lower left) and phase (lower right) of the reflection coefficient as a function of frequency for two different meshes. Results for the semi-empirical model is included

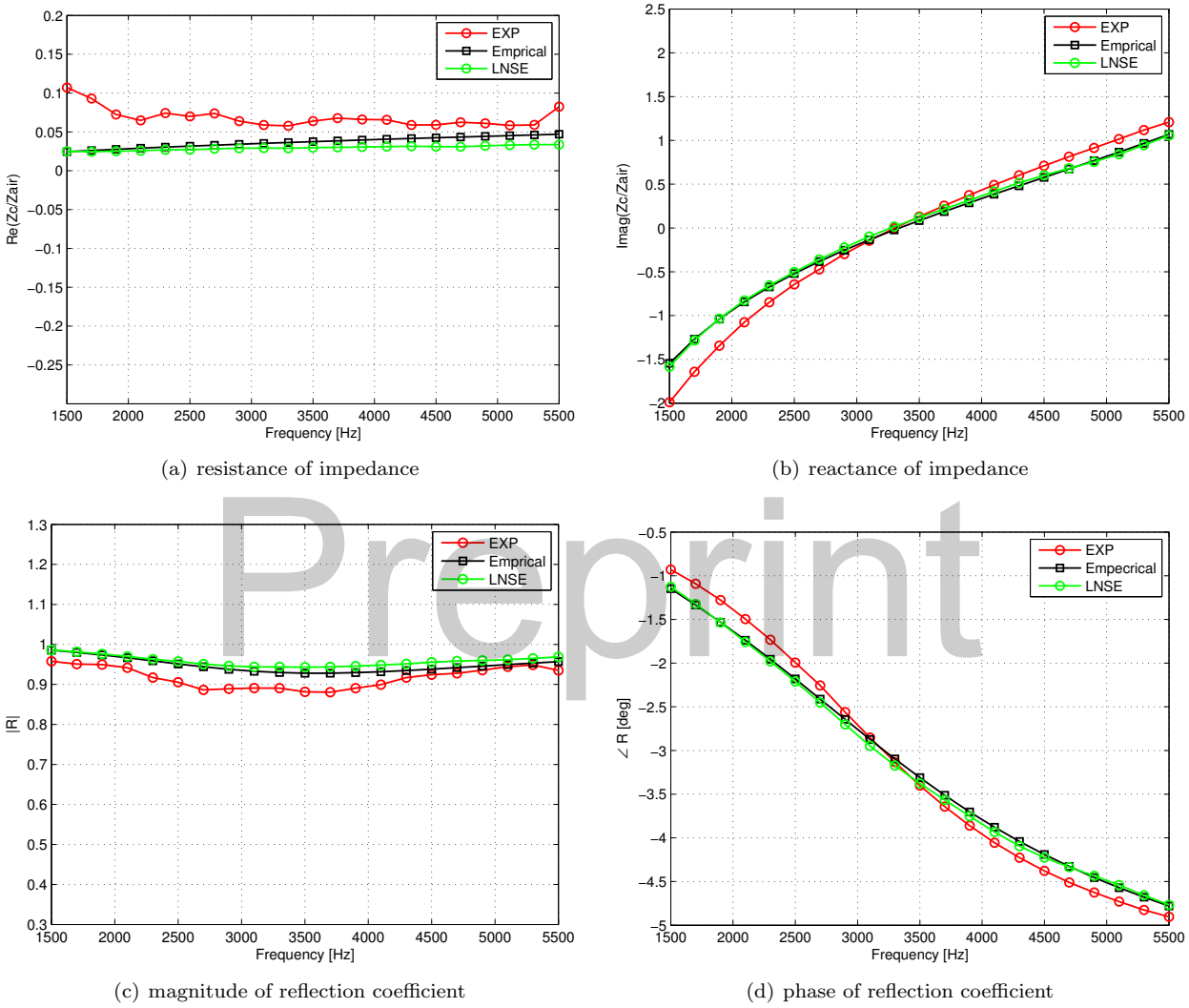

(a) resistance of impedance

(b) reactance of impedance

(c) magnitude of reflection coefficient

(d) phase of reflection coefficient

Figure 6. Resistance (upper left), reactance (upper right) and the magnitude (lower left) and phase (lower right) of the reflection coefficient as a function of frequency. Results for the semi-empirical model as well as experimental data is included.

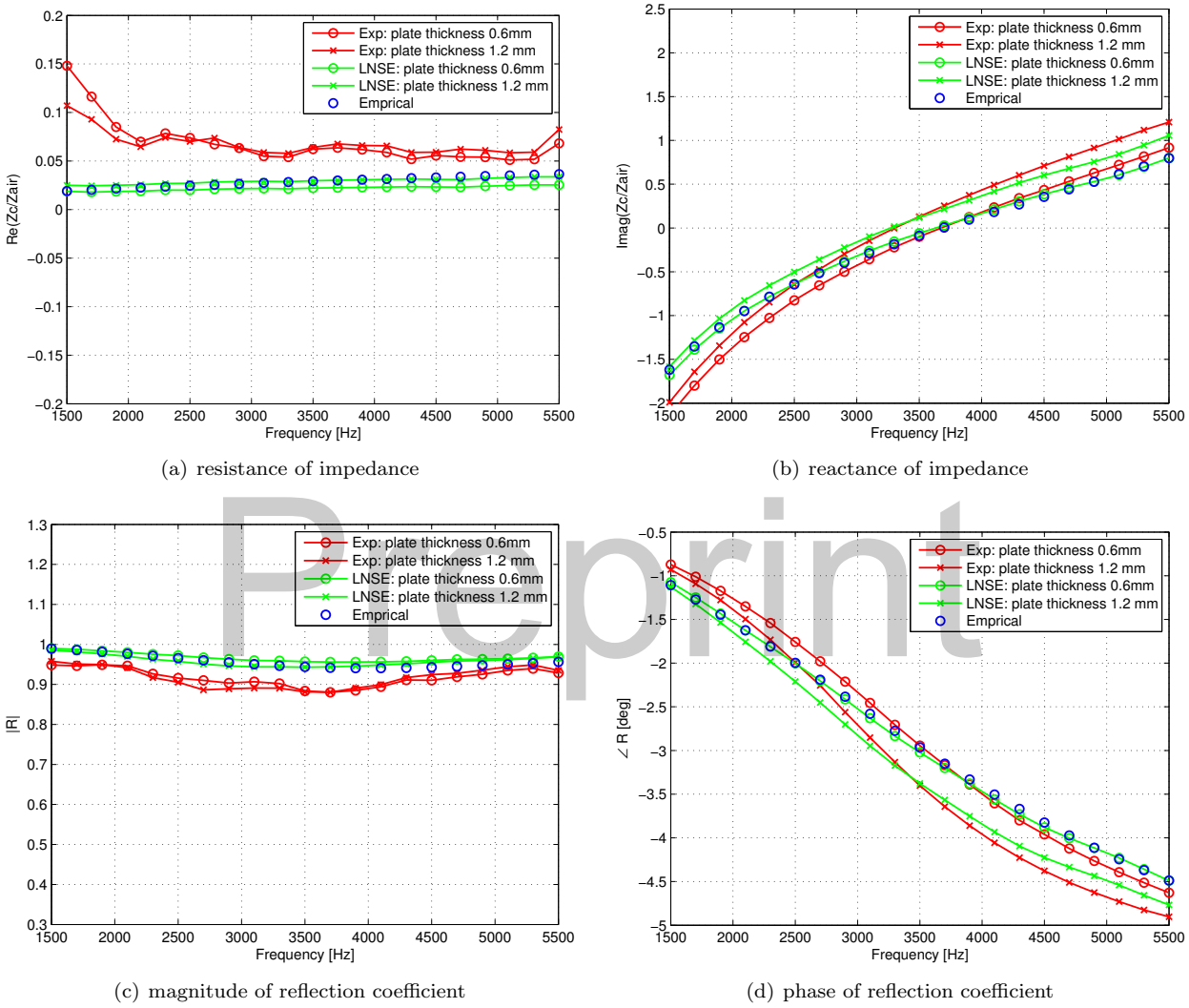

(a) resistance of impedance

(b) reactance of impedance

(c) magnitude of reflection coefficient

(d) phase of reflection coefficient

Figure 7. Resistance (upper left), reactance (upper right) and the magnitude (lower left) and phase (lower right) of the reflection coefficient as a function of frequency for two different porosities thicknesses. Results for the semi-empirical model and experimental data is included.

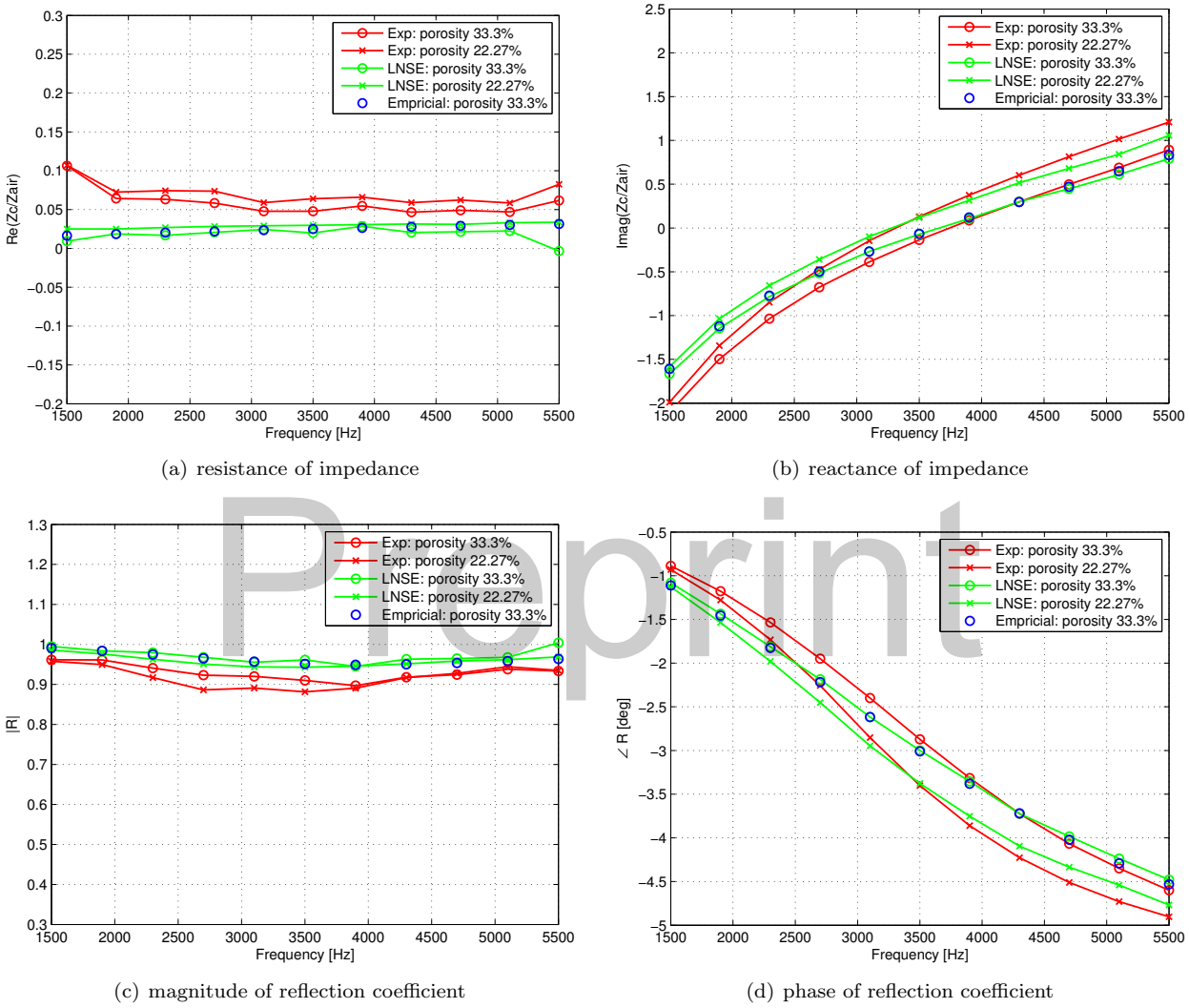

(a) resistance of impedance

(b) reactance of impedance

(c) magnitude of reflection coefficient

(d) phase of reflection coefficient

Figure 8. Resistance (upper left), reactance (upper right) and the magnitude (lower left) and phase (lower right) of the reflection coefficient as a function of frequency for two different porosities. Results for the semi-empirical model and experimental data is included.

VI. Conclusion

In this paper we have presented numerical results of the impedance and reflection coefficient for a liner consisting of a perforated plate and a rectangular back cavity using a linearized Navier-Stokes solver in frequency domain. The computational domain consisted of one cavity with 6 or 9 holes in the perforated plate. Studies on the sensitivity of the mesh resolution, as well as liner parameters such as plate thickness and porosity were shown. All results are compared to experimental results performed at KTH, see also the paper by Kabral et al,[7] and a semi-empirical model by Bauer.[15] It is seen that simulated results are in excellent agreement with the results by the semi-empirical model. The phase of the reflection coefficient agrees very well with the experimental results as well as the reactance calculated from the simulated results for low values of the reactance, that is in the region where the resonance frequency of the liner is expected to be found. Further analysis of the potential for the solver to be used for prediction of the resonance frequency will be performed in future studies. For all cases, the reactance from the simulated results are lower than those based on the experimental results. The reason for this could possibly be due to non-linear effects in the experimental data, which is not captured by the linear solver. In the present paper, the number of holes per back cavity cell were the same as in the experiments. In future work, we will also perform simulations of one cell with the same open area as for a six hole case.

Acknowledgments

The authors would like to thank Raimo Kabral and Hans Boden for generously sharing the experimental results and for all fruitful discussions on the similarities and discrepancies of the results.

The third author was financed by the Clean Sky CfP project HOSTEL, project number 308265, which is gratefully acknowledged. Further, the presented work is also a part of the Marie Curie Initial Training Network Thermo-acoustic and aero-acoustic nonlinearities in green combustors with orifice structures (TANGO). We gratefully acknowledge the financial support from the European Commission under call FP7-PEOPLE-ITN-2012.

The simulations were performed at the facilities within the PDC centre for high performance computing, KTH Stockholm.

References

[1]Tam, C., Kurbatskii, K., Ahuja, K., and JR., R. G., "A numerical and experimental investigation of the dissipation mechanisms of resonant acoustic liners," *Journal of Sound and Vibration*, Vol. 245, No. 3, 2001, pp. 545 – 557.

[2]Bodén, H. and Åbom, M., "Influence of errors on the two-microphone method for measuring acoustic properties in ducts," *The Journal of the Acoustical Society of America*, Vol. 79, No. 2, 1986, pp. 541–549.

[3]Åbom, M. and Bodén, H., "Error analysis of two-microphone measurements in ducts with flow," *The journal of the acoustical society of America*, Vol. 83, No. 6, 1988, pp. 2429–2438.

[4]Tam, C. K., Ju, H., and Walker, B. E., "Numerical simulation of a slit resonator in a grazing flow under acoustic excitation," *Journal of Sound and Vibration*, Vol. 313, No. 3, 2008, pp. 449–471.

[5]Tam, C. K., Ju, H., Jones, M. G., Watson, W. R., and Parrott, T. L., "A computational and experimental study of resonators in three dimensions," *Journal of Sound and Vibration*, Vol. 329, No. 24, 2010, pp. 5164–5193.

[6]Zhang, Q. and Bodony, D. J., "Numerical investigation and modelling of acoustically excited flow through a circular orifice backed by a hexagonal cavity," *Journal of Fluid Mechanics*, Vol. 693, 2012, pp. 367–401.

[7]Kabral, R., Lin Zhou, H. B., and Elnady, T., "Determination of liner impedance under high temperature and grazing flow conditions," *18th AIAA/CEAS Aeroacoustics Conference*, 2012.

[8]Kierkegaard, A., Boij, S., and Efraimsson, G., "A frequency domain linearized Navier-Stokes equations approach to acoustic propagation in flow ducts with sharp edges," *The Journal of the Acoustical Society of America*, Vol. 127, No. 2, 2010, pp. 710–719.

[9]Kierkegaard, A., Allam, S., Efraimsson, G., and Åbom, M., "Simulations of whistling and the whistling potentiality of an in-duct orifice with linear aeroacoustics," *Journal of Sound and Vibration*, Vol. 331, No. 5, 2012, pp. 1084–1096.

[10]Kierkegaard, A., Boij, S., and Efraimsson, G., "Simulations of the scattering of sound waves at a sudden area expansion," *Journal of Sound and Vibration*, Vol. 331, No. 5, 2012, pp. 1068 – 1083.

[11]Kierkegaard, A., Efraimsson, G., and Agarwal, A., "Simulations of a Liner Cell Using a Frequency-Domain Linearized Navier-Stokes Methodology," *19th AIAA/CEAS Aeroacoustics Conference*, 2013.

[12]Na, W., Efraimsson, G., and S.Boij, "Simulations of the scattering of sound waves at a sudden area expansion in a 3d duct," *ICSV 21: The 21st International Congress on Sound and Vibration*, 2014.

[13]Allam, S. and Åbom, M., "Investigation of damping and radiation using full plane wave decomposition in ducts," *Journal of sound and vibration*, Vol. 292, No. 3, 2006, pp. 519–534.

[14]Pierce, A. D., "Acoustics-An introduction to its physical principles and applications," *Physics Today*, Vol. 34, No. 12, 1981, pp. 56–57.
[15]Bauer, A. B., "Impedance theory and measurements on porous acoustic liners," *Journal of Aircraft*, Vol. 14, No. 8, 1977, pp. 720–728.